FREIA Report 2016/03
March 2016

UPPSALA UNIVERSITET

DEPARTMENT OF PHYSICS AND ASTRONOMY
UPPSALA UNIVERSITY

Giant single-cycle THz pulses for pump-probe experiments

Vitaliy Goryashko

FREIA, Department of Physics and Astronomy,
Uppsala University, Sweden

Department of
Physics and Astronomy
Uppsala University
P.O. Box 516
SE – 751 20 Uppsala
Sweden

Papers in the FREIA Report Series are published on internet in PDF- formats.
Download from http://uu.diva-portal.org

Giant single-cycle THz pulses for pump-probe experiments

ABSTRACT: Strong-field single-cycle THz pulses are an invaluable tool for probing and controlling low-energy excitations in matter such as magnons, plasmons, phonons and Josephson waves. A novel scheme is proposed to generate quasi-half-cycle GV/m THz pulses with a mutli-kilohertz repetition rate. It makes use of coherent spontaneous emission from a pre-bunched electron beam traversing an optimally tapered undulator. The scheme is the further development of the novel concept of the slippage control in free-electron lasers [T. Tanaka, PRL 114 (2015) 044801]. The pump-probe configuration THz/X-ray/optical is discussed.

1. INTRODUCTION

The spectral range of THz radiation corresponds to collective excitations in multi-atomic systems such as molecular rotations, DNA dynamics, spin waves, Josephson waves and phonons. Strong-field THz pulses allow engineering new dynamic states of matter by selective excitation of the process of interest. One of the non-trivial examples of new physics discovered with intense THz light is the excitation of a transient Josephson plasma wave in superconducting cuprates significantly above the critical temperature of the sample. This phenomenon is indicative of the possibility of room temperature superconductivity.

THz photons are highly advantageous in comparison with optical ones, which often contain excessive energy relative to the type of low-energy resonances given above. Superfluous energy from the optical photons may, for example, be distributed as phonon excitations or hot electron distributions, which result in less control and unwanted temperature increase. In contrast, the THz pulse provides a fine stimulus that allows targeting the excitation of interest and thus opening the door to controlled manipulation of reactions and processes.

A flexible strong-field THz light source is required for studying fundamental collective excitations. Here I present a design of a THz light source delivering quasi-half-cycle or multi-cycle THz pulses with a field strength in the V/Å range at a multi-kilohertz repetition rate. It makes use of coherent spontaneous radiation from pre-bunched electron beams and a new concept of slippage control between electrons and the radiated field. With respect to other THz light sources the proposed Light Source in Uppsala has a number of unique features:

- it is designed specifically for pump-probe experiments;
- the broadband THz source will cover the range from 5 to 15 THz, where laser-based THz sources fail to work;
- the THz source will generate quasi-half-cycle pulses with field strength and repetition rate that are far beyond any existing or planned source.

2. LAYOUT OF THE BASELINE DESIGN

The key part of the design is two THz sources that can deliver either GV/m quasi-half-cycle or intense narrowband THz pulses. The first source makes use of the recently proposed Tanaka scheme [1] for generation of isolated monocycle radiation from a tapered undulator. Tanaka's scheme was originally proposed for the generation of attosecond X-ray pulses, so in our design it is properly modified for the generation THz pulses. The basic idea is that a train of electron microbunches emits a train of frequency-chirped THz pulses in the tapered undulator, and by a proper choice of the period between the microbunches one can obtain a wavepacket that has constructive interference of individual pulses at its center whereas at the tails the pulses are cancelled out by destructive interference. The resulting wavepacket can be as short as one cycle and a half with a field strength of GV/m and even more with focusing. A great advantage of such a source over a CTR source is its linear polarization of the field.

The narrowband THz pulses are generated in a regular undulator by a pre-bunched electron beam, whose period of modulation is equal to that of undulator radiation. Provided that microbunches are sufficiently short, intense coherent spontaneous radiation (often referred to as superradiant) is emitted by each microbunch and the total emitted energy is proportional to the beam charge squared that can be as high as a nC. In such a configuration, there is no need to compress the whole beam to 100 fs scale, which removes constrains on the beam charge pertinent to other facilities using a non-modulated beam. The pre-bunched beam is formed in an RF gun by making use of a train of laser pulses to extract electrons from a photo-cathode.

The regular undulator is followed by a single-period undulator that produces a broadband THz probe in the form of a train of single-cycle pulses, which permits stroboscopic measurements. The narrowband pump and broadband probe are naturally synchronized since they produced by the same beam. The delay between the pump and probe can be adjusted by the path length travelled by the narrowband pulse.

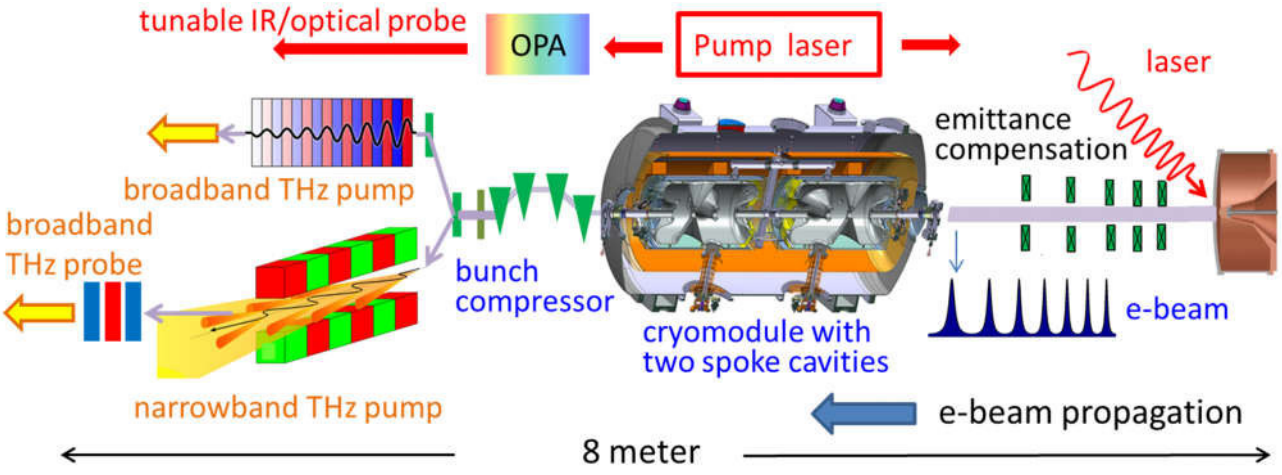

Fig. 1: Layout of the pump-probe source.

Apart from the pump-probe capabilities of the THz sources, we will also provide users with a powerful optical pump and tunable IR/optical probe. To this end, a combination of a pump laser and an optical parametric amplifier (OPA) will be used. Part of the pump laser pulse will be split out in order to drive the photocathode.

Some applications require an X-ray source for time-resolved diffraction studies. Such a source is not part of the baseline design but can be installed on the users' request. One of the optimal options for generation of narrowband X-ray radiation is the Compton scattering of laser pulses on electron bunches. The collision of electrons in the energy range from 10 to 20 MeV with a 1 μm laser pulse will result in X-ray scattered photons in the range from 2 to 8 keV (2-7 Å). Upon collision of a train of 50 fs, 100 pC electron bunches with 200 fs, 1 mJ laser pulses, around $5*10^3$ photons will be produced per bunch per shot, with the total number of photons of around 10^6 per second into 0.1% bandwidth. This is comparable to the synchrotron slicing source with its 10^5-10^7 photons per second into 0.1% BW. After the Compton source, electron bunches are sent to one of the THz sources described above.

3. THE ACCELERATOR

The THz light source will be based on a superconducting linear accelerator (linac) to provide a CW mode of operation with a repetition rate from 1 up to 100 kHz with evenly spaced pulses. The spoke cavities are a good choice for such a linac with their small wakefields due to large apertures, weak cavity sensitivity to microphonics and highly efficient solid-state RF sources at low frequencies to drive the cavities. We expect the cavities to be operated at 10 MV/m giving more than 20 MeV energy gain from two cavities. It should be noted that the operation of beta 0.5 spoke cavities at a gradient of 13 MV/m was recently demonstrated at the FREIA laboratory.

The electron gun is the most crucial component of the linac and currently we are considering two options: a low-frequency normal conducting photocathode gun similar to the APEX gun developed for LCLS-II and a superconducting (SC) photocathode gun. The latter gives higher accelerating gradient so that bunches with more charge can be delivered, however, at higher expense and complication in operation. In order to generate a pre-bunched electron beam for further generation of superradiant THz pulses, a train of 200 fs laser pulses with a period of 0.5-1 ps will illuminate the photocathode to drive electrons out of it. Each laser pulse will result in a 100 pC electron bunch with 12-15 bunches in total. The electron beam will have an energy of around 0.5 MeV and 1 μm emittance.

After the gun, the beam enters an emittance compensation line in the form of a drift with properly profiled magnetic field followed by two superconducting cavities, and a bunch compressor. The compression factor is around 5 and 20 MeV electron bunches will be just 50 fs long with 100-200 fs separation. Then, the beam is directed to the Compton source or one of the THz sources.

4. GENERATION OF SINGLE-CYCLE GV/M THZ PULSES

Presently, ultra-short THz pulses are mainly generated via optical rectification of a short intense optical pulse (10-100 fs) that drives a nonlinear polarization through the second order nonlinear susceptibility in crystal such as LiNbO3. The current record for the generated energy is 125 uJ, but the radiation spectrum is mostly limited to 1.5 THz [2]. Broadband THz radiation is also available through two-color laser mixing in air plasma. However, the emitted energy is limited to several nJ with a low conversion efficiency of 10^{-4} from optical to THz energy, and the repetition rate is only up to a kHz [3]. Yet another method for generation of high-cycle THz pulses is transition radiation from high-energy charged particles traversing a metallic foil. This method allows generating by far the most intense THz pulses with electric field strength up to 1 GV/m (atomic fields!) that exceeds at least by one order of magnitude all other sources. However, this method can be applied only at large accelerating facilities since it requires multi-GeV electron bunches of a few nC charge. Currently, the only source of that kind producing 1 GV/m THz pulses is available at the FACET facility of SLAC and makes use of the SLAC copper linac to accelerate 2.5 nC bunches to 23 GeV [4]. The repetition rate is limited to around 100 Hz. In order to overcome the deficiency of low conversion rate of the electron beam energy into radiated energy of transition radiation, a multifoil cone radiator [5] was suggested with a promise to boost the emitted energy by one order of magnitude of more. However, the repetition rate is estimated to be limited to a kHz because of heat load on the radiator. *None of the conventional methods meets the objective set by the users' demand*. Therefore, in the baseline design we will use a modified version of recently proposed Tanaka's method [1] for generation of an isolated monocycle radiation with a tapered undulator.

Tanaka's idea is as follow: consider a tapered undulator such that the period of the EM pulse emitted by a test electron traversing the undulator monotonically changes along the pulse, *i.e.* the pulse is frequency-chirped. Suppose we generated a pre-bunched electron beam whose period changes in the same way as that of the EM pulse. Then, the combined pulse is a wavepacket composed of identical wavefronts shifted by one period with respect to each other and interfering constructively at the center of the wavepacket and destructively at the tails, see the illustration of the idea in Fig. 2. It is shown in [1] that the resulting field, which is the convolution of the field emitted by one electron and the current density, is $E(t) = bn_0E_0 \quad ^{-1}[|f_\omega|^2]$, where $^{-1}$ stands for the inverse Fourier transform, f_ω is the Fourier transform of the temporal profile $f(t)$ of the EM pulse of magnitude E_0 emitted by a test electron; b and n_0 are the bunching factor and average electron density, respectively. By employing an undulator with a large taper rate one can have broadband undulator emission and, therefore, short pulses from a pre-bunched electron beam.

In order to form the required pre-bunched beam, Tanaka suggested using a modulator-undulator that is an undulator identical to the one used for generation of broadband radiation but with reserved tapering. In the original scheme a seed is provided by an external laser but at THz frequencies it is more efficient to use a seed electron bunch that follows the main bunch and is sufficiently short to generate coherent spontaneous radiation in the modulator, which is further downstream used to imprint the required temporal modulation to the main bunch. One more option of forming the pre-bunched beam is via direct laser shaping of the beam at a cathode. It has great potential and will be given further careful consideration.

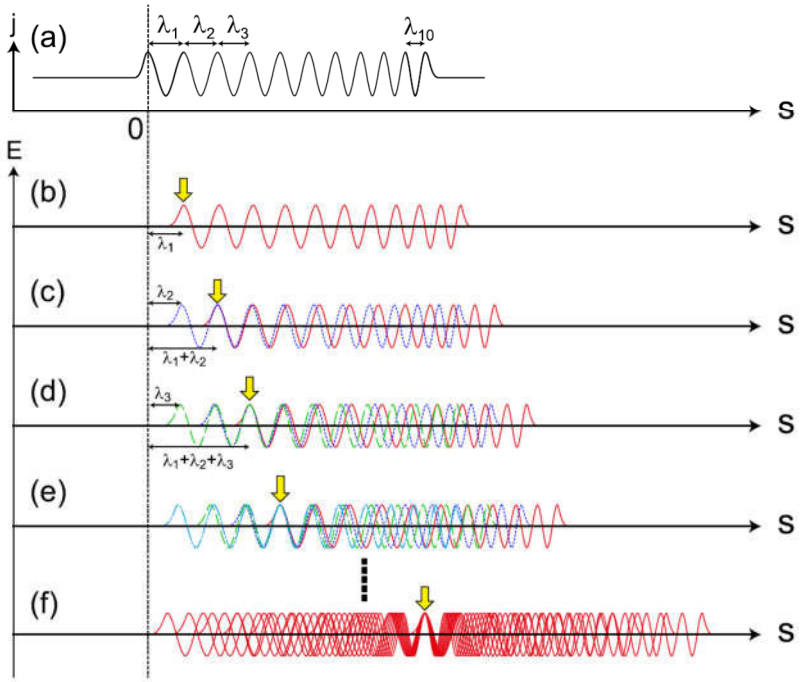

Fig. 2: To the explanation of the generation of isolated monocycle radiation (adopted from [1]).

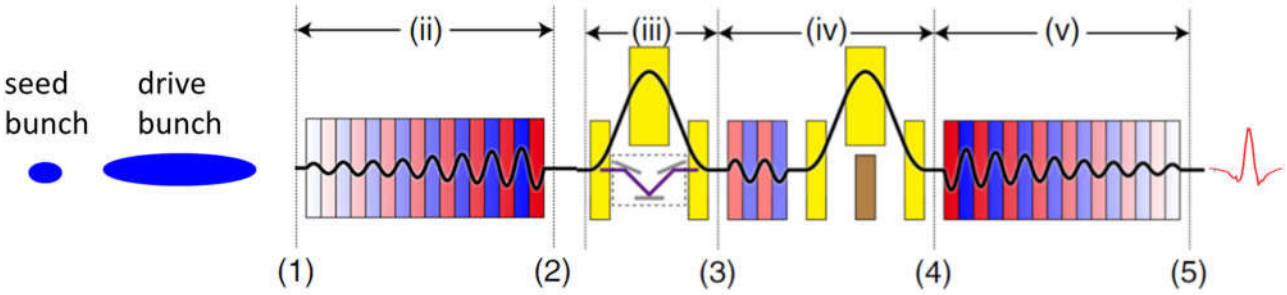

Fig. 3: Modified configuration of Tanaka's scheme.

5. QUASI-HALF-CYCLE PULSES FROM A TAPERED UNDULATOR

The wavelength of the field radiated by a test electron traversing an undulator with a field envelope $f_u(z)$ reads

$$\lambda = \frac{\lambda_u}{2\gamma^2}\left(1 + \frac{\mathcal{K}^2}{2} f_u^2(z)\right), \tag{1}$$

where λ_u and $\mathcal{K}$ are the period and conventional undulator parameter, respectively; γ is the electron's energy in units of the rest mass. The magnitude of the undulator magnetic field B_0 is related to $\mathcal{K}$via $\mathcal{K} = 0.934\, B_0[\text{Tesla}]\lambda_u[\text{cm}]$. The radiation wavelength changes along the undulator and by employing profiling with a large amplitude variation one can generate very broadband radiation. We aim at generating quasi-half-cycle pulses with the temporal profile of the form

$$A(t) = A_0 \left(1 \quad \frac{t^2}{\sigma_t^2}\right) \exp\left[\quad \frac{t^2}{2\sigma_t^2}\right], \tag{2}$$

depicted in Fig. 4.

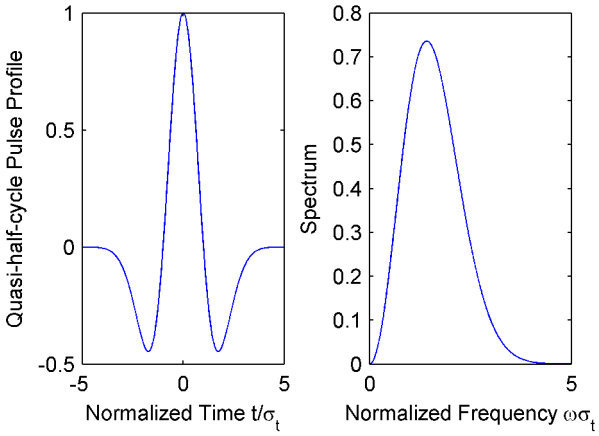

Fig. 4: The temporal profile and spectrum of quasi-half-cycle pulses.

The first step is to optimize the undulator tapering. Using the conventional quasi-1D approach within which the electron bunch is treated as a collection of charged slices performing undulator oscillations in the transverse of longitudinal directions, we found the complex spectral component of the co-propagating electric field to read

$$E_\omega = E_\omega^0 \int_0^{L_u} g(z') e^{i\Psi(z')} dz', \tag{3}$$

where the field amplitude is

$$E_\omega^0 = \quad \frac{Q_b}{cS_b}\frac{\mathcal{K}}{\gamma} e^{-\omega^2\sigma_T^2/2}, \tag{4}$$

$g(z) = f_u(z)JJ(z)$, JJ stands for the well-known JJ-factor

$$JJ = J_0(A) \quad J_1(A), \qquad A = \frac{\mathcal{K}^2 f_u^2(z)}{4\xi} \tag{5}$$

and the ponderomotive phase is

$$\Psi = \frac{2\pi}{\xi\lambda_u}\left[z(1 \quad \xi) + \frac{\mathcal{K}^2}{2}\int_0^z f_u^2(z')dz'\right]. \tag{6}$$

Here, $Q_b$and S_b are the bunch charge and transverse area, respectively; σ_T is the bunch duration; L_u is the undulator length; c is the speed of light in vacuum; $J(A)$ is the Bessel function of the first kind; $\xi = \lambda/\lambda_0$ is the normalized wavelength with $\lambda_0 = \lambda_u/2\gamma^2$ being the Doppler-upshifted period of the undulator field. The electric field in the time domain is given by

$$E(z,t) = \mathrm{Re}\int_0^\infty E_\omega(z)\, e^{-i\omega(t-z/c)} d\omega. \tag{7}$$

Integral (3) can be solved using the method of stationary phase in the same manner as it is done in the studies of Thompson backscattering of lasers pulses on electron bunches. The main

contribution to the integral comes from the so-called stationary point, in the vicinity of which phase Ψ is quasi-constant. Otherwise, if the change in Ψ over the integration region is much greater than π, then the contributions of the integrand from different points cancel out each other to a large extent since the factor in front of the exponential is a slow function of z and basically we integrate a sinusoidal function multiplied by a slow-varying amplitude. The solution to Eq. (3) for *non-degenerated* stationary points $\Psi''(z_0) \neq 0$ reads

$$E_\omega \approx \sum_j \sqrt{\frac{2\pi}{\Psi''(z_{0,j})}} E_\omega^0 g(z_{0,j}) \exp\left[i\Psi(z_{0,j}) + i\frac{\pi}{4}\mathrm{sgn}\Psi(z_{0,j})\right], \tag{8}$$

where the symbol prime stands for the derivative with respect to z. The point of stationary phase z_0 is determined by the condition $\Psi'(z_0) = 0$, and the summation is over all stationary points that are within the integration interval and located from the ends of the interval at a distance greater than the width of the corresponding resonance. Asymptotic solution (8) is obtained from Eq. (3) by Taylor expanding phase Ψ around point z_0 up to the second order and integrating only the exponential while the term $g(z)$ is factored out at point z_0 thanks to its slow dependence on z. The explicit equation determining stationary points reads

$$\xi = 1 + \mathcal{K}^2 f_u^2(z_0)/2 \tag{9}$$

and solutions to it exist for wavelengths ranging from $\xi_{\min} = 1 + \mathcal{K}^2 \min f_u^2\,/2$ to $\xi_{\max} = 1 + \mathcal{K}^2 \max f_u^2\,/2$.

If the undulator profile $f_u(z)$ is symmetric, then in the region $\xi \in (\xi_{\min}, \xi_{\max})$ condition (9) is satisfied for two positions in the undulator and the spectral component (8) is the sum of two waves with the same frequency but different phases. Such a superposition results in oscillations in the spectrum of emitted radiation. In order to avoid these oscillations, the undulator profile must be a monotonic function of z. The optimal undulator profile can be found by equating the spectral density of undulator radiation $|E_\omega|^2$ to the spectral density of the quasi-half-cycle pulse $|A_\omega|^2$ and solving the resulting equation. In order to simply the analysis, it is advantageous to Taylor expand $|A_\omega|^2$ in the vicinity of its maximum. In this way, we obtain the first-order differential equation for f_u

$$\frac{f_u \xi}{f_u'} = L_{\mathrm{ef}}[1 \quad (\xi \quad 2)^2], \tag{10}$$

where L_{ef} is the parameter of the dimension of length. By eliminating ξ via $1 + \mathcal{K}^2 f_u^2(z_0)/2$ and separating the variables, one can integrate the above equation to obtain the relation

$$\frac{z}{L_{\mathrm{ef}}} = \frac{3}{2}\log\left[1 + \frac{f_u^2 \mathcal{K}^2}{2}\right] \quad \frac{f_u^2 \mathcal{K}^2}{4}, \tag{11}$$

whose solution can be obtained by fitting numerically a polynomial for given $\mathcal{K}$. The cubic fit for $\mathcal{K} = 2$ reads

$$f_u(z) = 5.4\left(\frac{\zeta z}{L_u}\right)^3 + 5\left(\frac{\zeta z}{L_u}\right)^2 + 2.4\left(\frac{\zeta z}{L_u}\right). \tag{12}$$

The parameter ζ is equal to 0.65 and in numerical simulations it can be adjusted to improve the spectral distribution. Numerically, we found that the optimum value of ζ is 0.7.

In order to check how efficient the found optimal profile is, we developed a quasi-1D self-consistent simulation code that solves the equations of charged slices and calculates the field from the 1D wave equation. First, we applied the code to the case of a bunch traversing a linearly tapered undulator. The results of simulations are depicted in Fig. 5 and the main parameters are summarized in Table I. The spectrum of emission from such an undulator is quite broad but not uniform and the field resulting from the superposition of waves emitted by an ideally pre-bunched beam is roughly 2 cycles long with long oscillating tails. In the first order approximation, the total field produced by a train of bunches is the superposition of wavefronts of individual bunches, hence, the simulation results for one bunch are used to find a resulting wavepacket assuming properly shaped bunches, *i.e.* assuming the beam profile to be identical to the field profile depicted in Fig. 5 on the top-right.

The use of the optimal tapering found analytically makes the spectrum more Gaussian-like and reduces the number of cycles to 1.5 while simultaneously reducing ringing, see the bottom-right plot in Fig. 6. The peak electric field is bit more than 1 GV/m and the emitted energy is around 3 mJ.

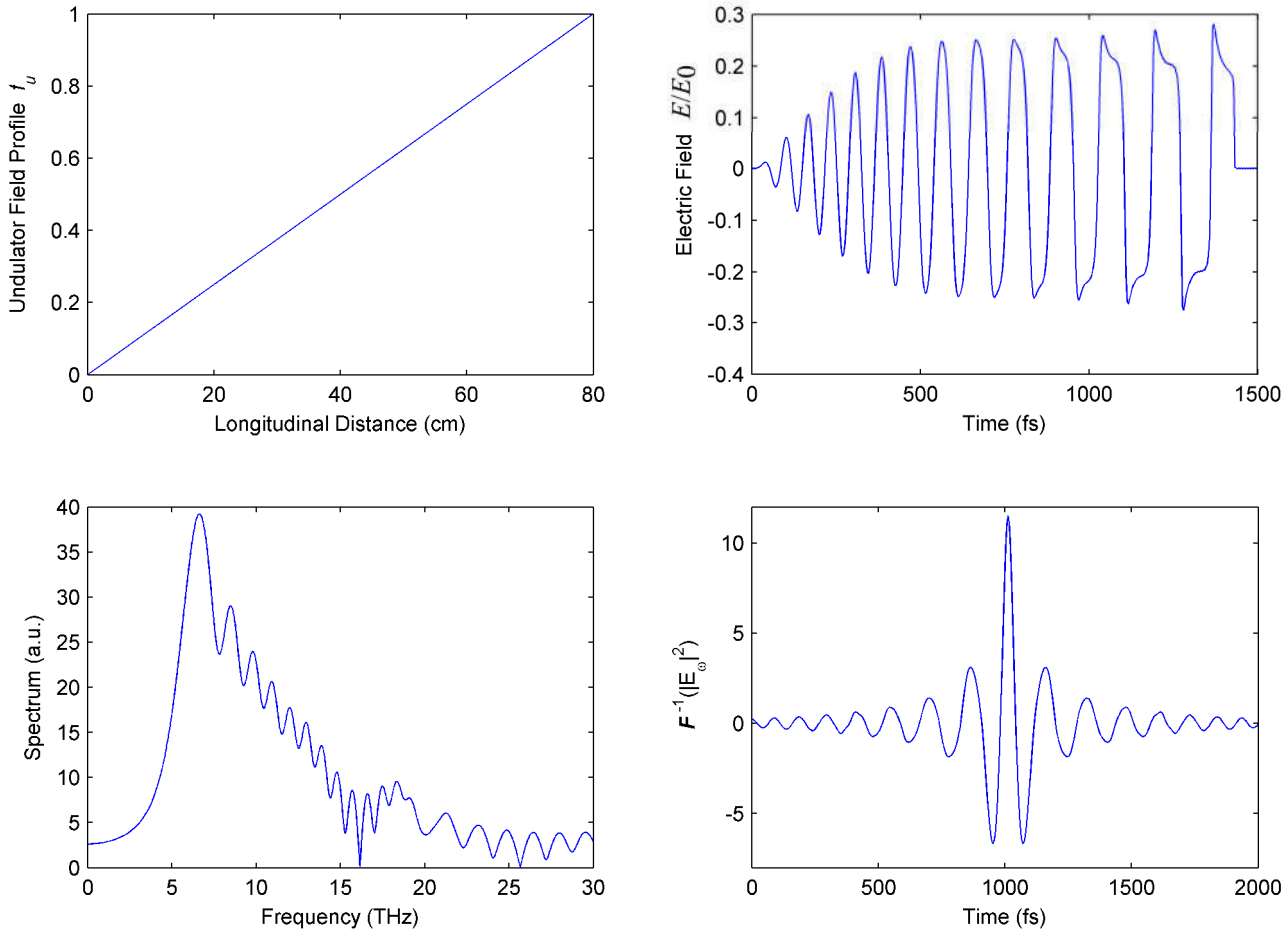

Fig. 5: The results of 1D simulations for a single microbunch. From the top left to the bottom right: profile of the undulator field; the electric field as a function of time; Fourier-transform of the electric field $|E_\omega|$ as a function of frequency; the combined electric field that would be produced by the ideally pre-bunched beam vs. time.

Table I: Main parameters of *single-bunch* broadband emission.

Parameter	Symbol	Value	Units
bunch charge	Q_b	100	pC
bunch duration	σ_τ	50	fs
bunch radius	r_b	1	mm
bunch energy	U_b	20	MeV
undulator period	σ_u	6	cm
number of periods	N_u	15	
undulator parameter	$\mathcal{K}$	2	
field normalization factor	E_0	288.5	MV/m
peak electric field	E_{peak}	80	MV/m
	linear taper		
emitted energy	$_r$	26	uJ
central frequency	f_c	7.25	THz
relative bandwidth	$\Delta\omega/\omega$	95%	
	optimal taper		
emitted energy	$_r$	25	uJ
central frequency	f_c	9	THz
relative bandwidth	$\Delta\omega/\omega$	105%	

Being convinced by the results of the 1D *self-consistent* simulation that the relative motion of charged slices caused by the radiation field is negligible and has no impact on the field itself, we developed a 3D simulation code that solves directly the 3D wave equation with a source in the form of a collection of charged slices whose shape and dynamics are governed by external magnetic fields. The results of 3D simulations are illustrated in Fig. 7 and 8. The on-axis electric field calculated with the help of the 3D model at the end of the optimally tapered undulator is almost identical to the field calculated within 1D model, Fig. 7. However, at a distance of 1 meter away from the undulator, the field profile is changed significantly by diffraction, Fig. 8, and the combined field from a perfectly pre-bunched beam not a quasi-half-cycle pulses since the undulator profile was optimize for the desired pulse shape at the end of undulator. Further optimization is needed to ensure the required field profile at a detector.

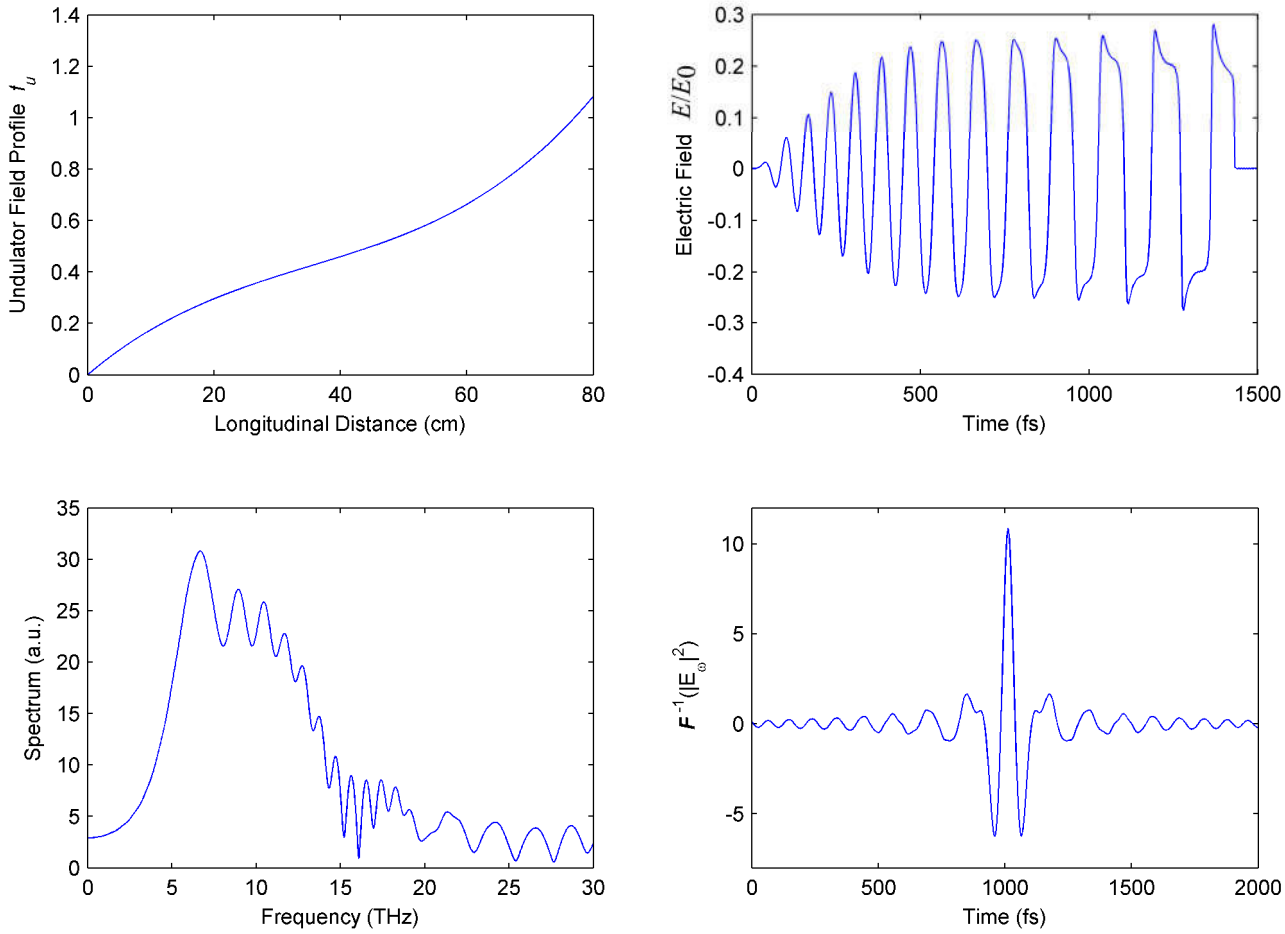

Fig. 6: The results of 1D simulations for a single microbunch. From the top left to the bottom right: profile of the undulator field; the electric field as a function of time; Fourier-transform of the electric field $|E_\omega|$ as a function of frequency; the combined electric field that would be produced by the ideally pre-bunched beam vs. time.

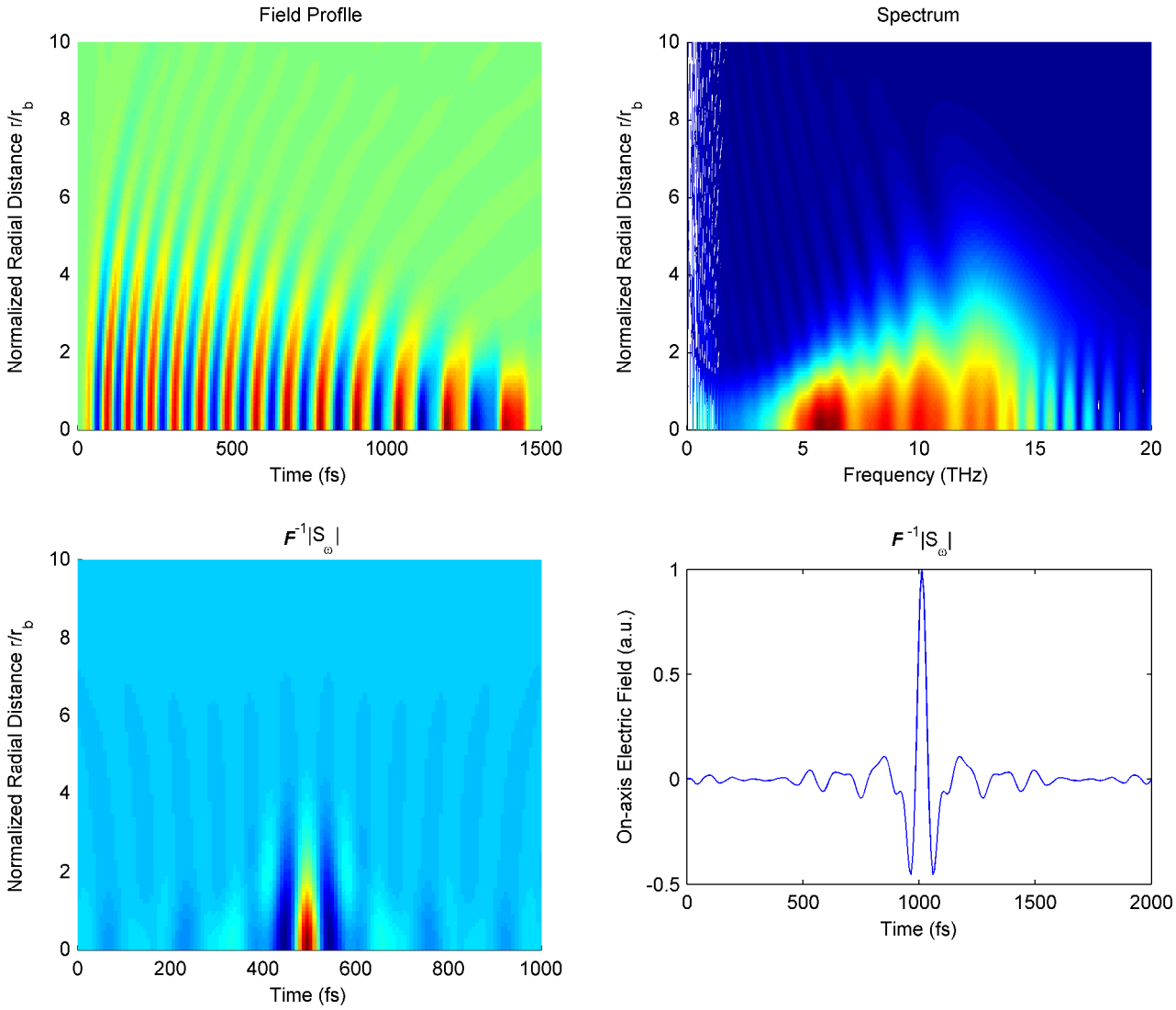

Fig. 7: The results of 3D simulations for a single microbunch. All characteristics are presented at the output of the optimally-profiled undulator. From the top left to the bottom right: the density plot of the electric field as a function of time and normalized radial distance; the density plot of $|E_\omega|$ as a function of frequency and normalized radial distance; the density plot of the combined electric field that would be produced by the ideally pre-bunched beam vs. time and normalized radial distance; on-axis combined field vs. time. The undulator profile was optimized for obtaining a quasi-half-cycle field at the output of the undulator.

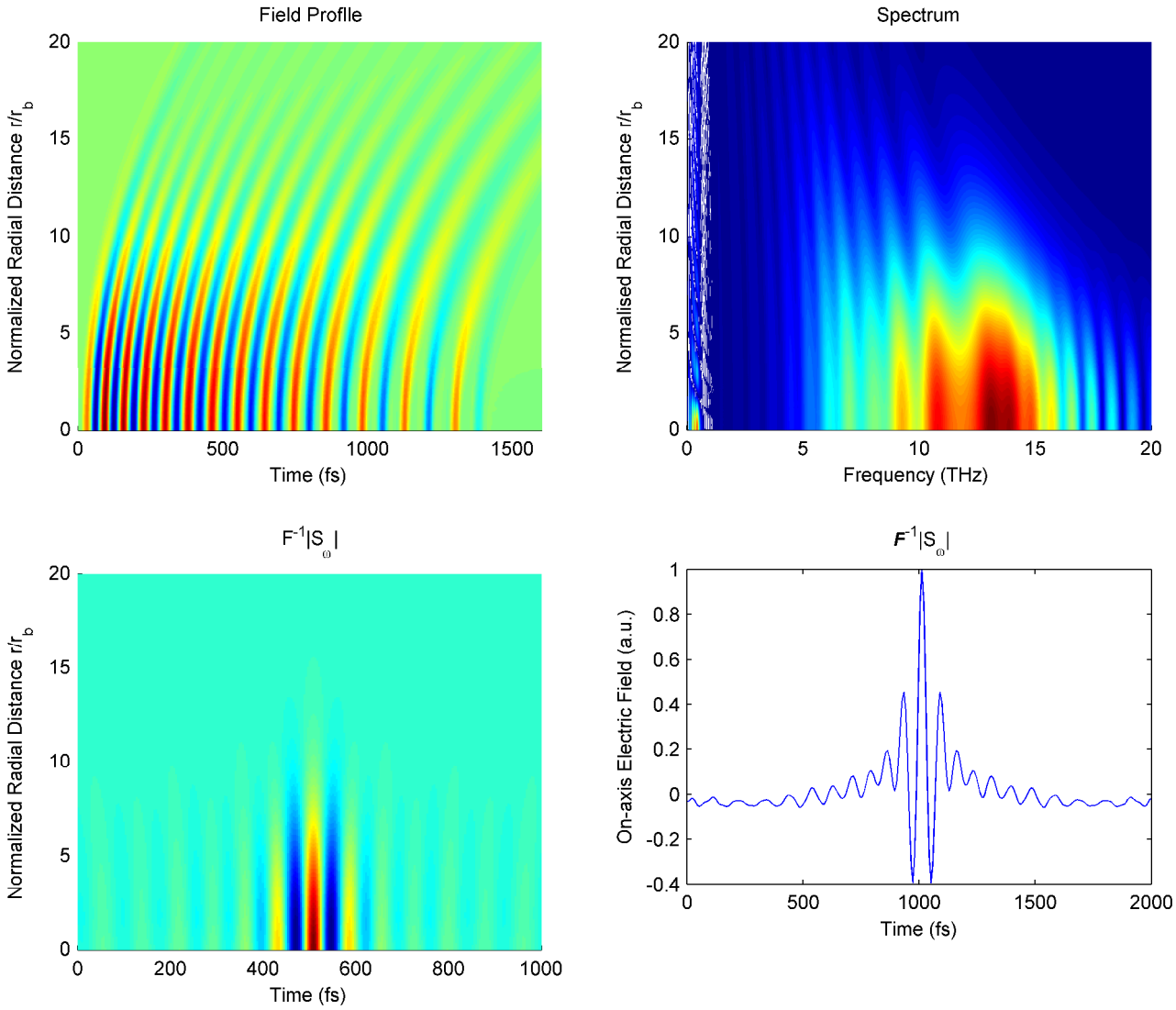

Fig. 8: The results of 3D simulations for a single microbunch. All characteristics are presented *at a distance 1 m away* from the optimally-profiled undulator. The undulator tapering is non-optimal for this distance. From the top left to the bottom right: the density plot of the electric field as a function of time and normalized radial distance; the density plot of $|E_\omega|$ as a function of frequency and normalized radial distance; the density plot of the combined electric field that would be produced by the ideally pre-bunched beam vs. time and normalized radial distance; on-axis combined field vs. time.

6. NARROW-BAND UNDULATOR EMISSION

Narrowband radiation needed as a pump pulse can be obtained by using a regular undulator and a pre-bunched electron beam. The results of 3D simulations are depicted in Fig. 9. As an example, we considered a 15-period undulator with the parameters summarized in the Table II. The simulation results are given at the end of the undulator and a distance of 1 m away from it. The peak electric field and total emitted energy from a beam composed of 15 bunches are around 0.9 GV/m and 4 mJ, respectively. Note that the total kinetic energy of the beam is 30 mJ, which implies the energy conversion of 13%. The field pattern of THz pulses can be quite well described by the fundamental optical beam with a Rayleigh length of around 45 cm.

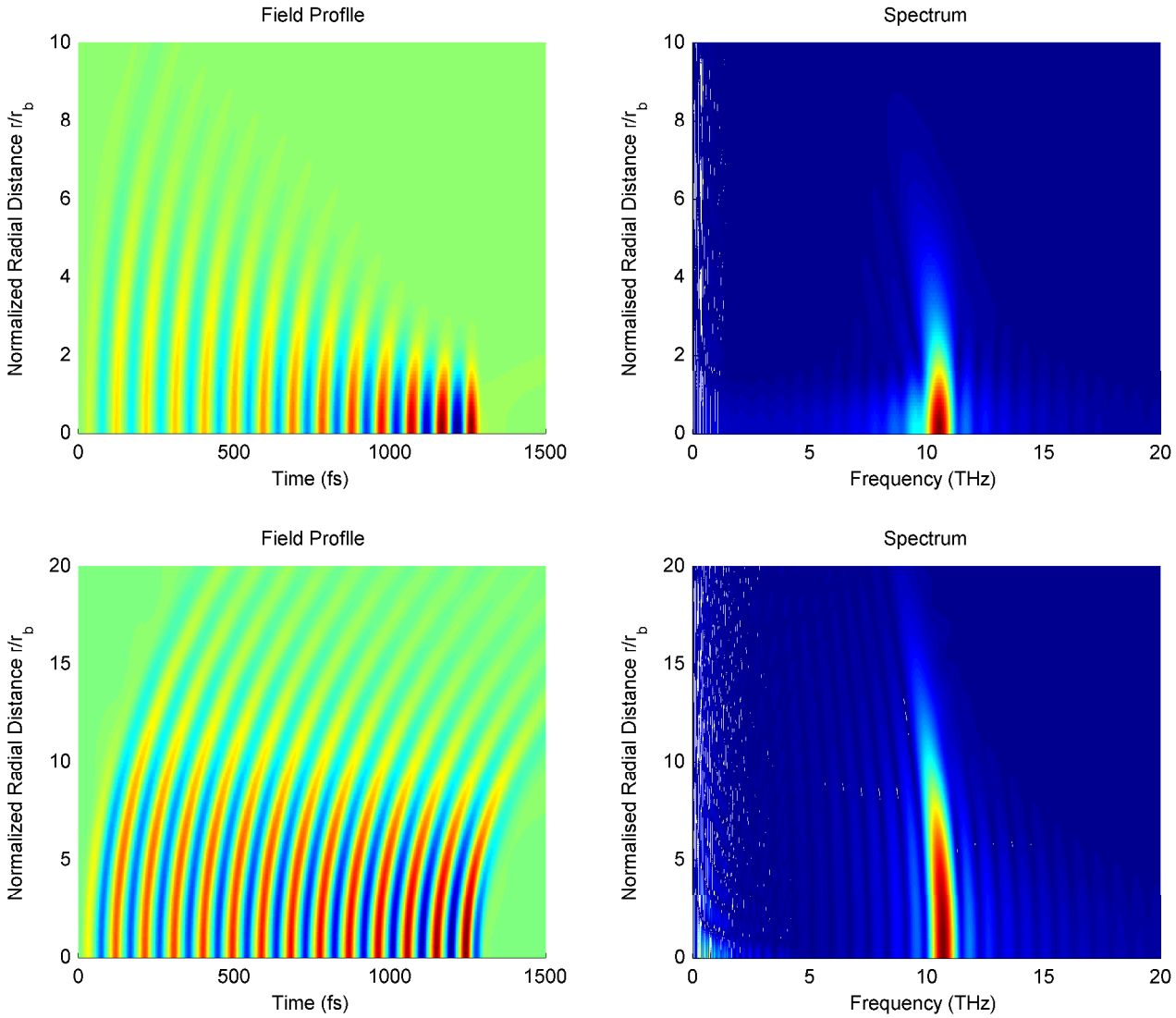

Fig. 9: The results of 3D simulations of emission from a single microbunch traversing a *regular* undulator. From the top left to the bottom right: the electric field and spectrum as a function of time and normalized radial distance at the end of undulator; the electric field and spectrum as a function of time and normalized radial distance at a distance of 1 m from the undulator.

Table II: Main parameters of *single-bunch* emission from a regular undulator.

Parameter	Symbol	Value	Units
bunch charge	Q_b	100	pC
bunch duration	σ_τ	50	fs
bunch radius	r_b	1	mm
bunch energy	U_b	20	MeV
undulator period	σ_u	6	cm
number of periods	N_u	15	
undulator parameter	$\mathcal{K}$	1	
peak electric field	E_{peak}	70	MV/m
emitted energy	$_r$	29	uJ
central frequency	f_c	10.52	THz
relative bandwidth FWHM	$\Delta\omega/\omega$	10%	

7. EMISSION FROM A SINGLE UNDULATOR SEGMENT

There is great interest in THz pump - THz probe experiments and in order to provide users with such type of capability there will be installed a single-period undulator next to the long one described above. The short undulator will produce 1.5 cycle 100 fs pulses in the spectral range from 3.4 to 15.6 THz (FWHM) and the central frequency of 8.5 THz. The main characteristics of the bunch, short undulator and resulting radiation are given in the Table III. It should be stressed that the bandwidth of radiation is almost 150%. The graphic illustration of the electric field profile and spectrum are presented in Fig. 10.

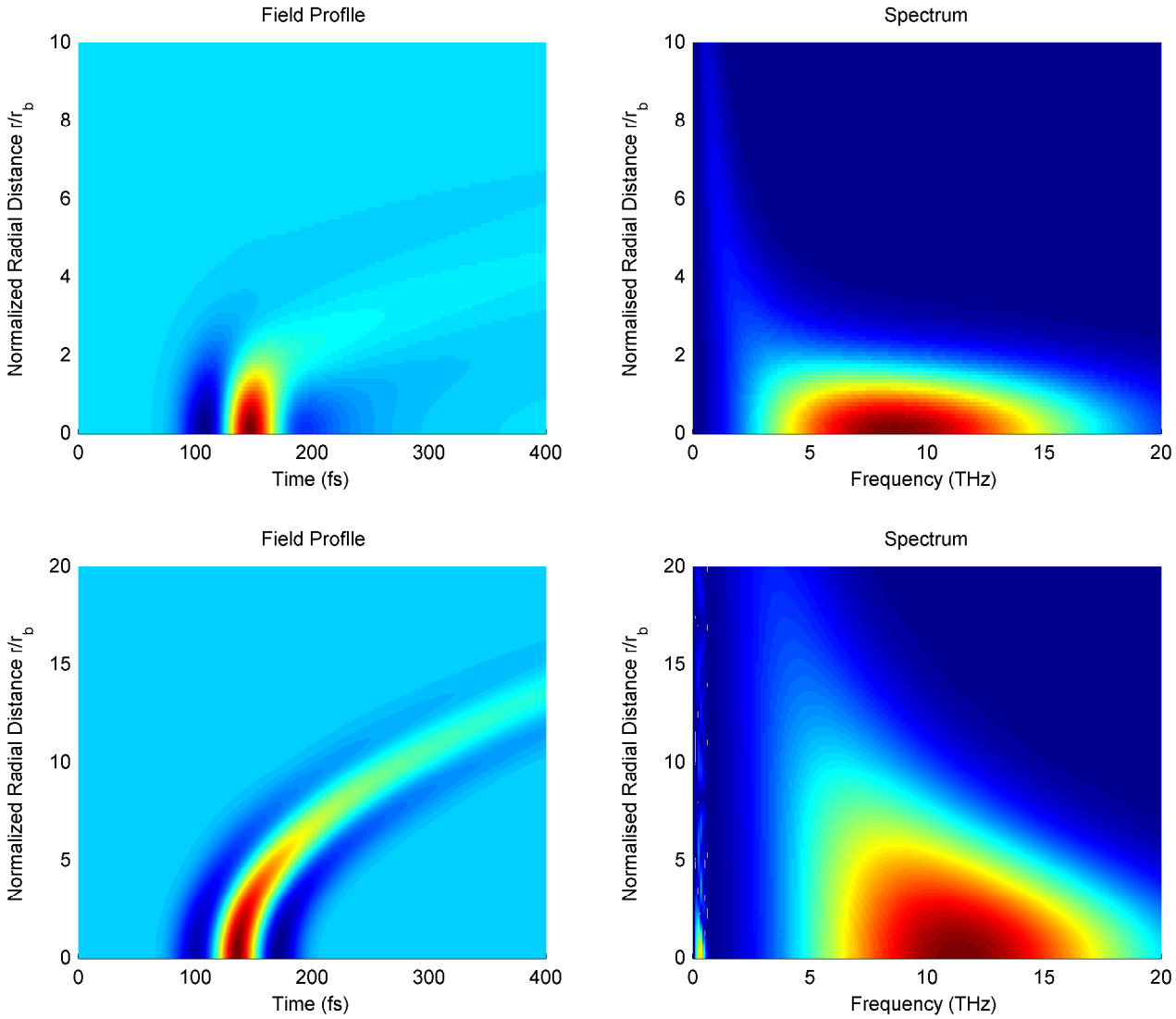

Fig. 10: The results of 3D simulations of emission from a single microbunch traversing a *one-period* undulator. From the top left to the bottom right: the electric field and spectrum as a function of time and normalized radial distance at the end of undulator; the electric field and spectrum as a function of time and normalized radial distance at a distance of 1 m from the undulator.

Table III: Main parameters of *single-bunch* emission from a one-period undulator.

Parameter	Symbol	Value	Units
bunch charge	Q_b	100	pC
bunch duration	σ_τ	50	fs
bunch radius	r_b	1	mm
bunch energy	U_b	20	MeV
undulator period	σ_u	1.5	cm
number of periods	N_u	1	
undulator parameter	$\mathcal{K}$	0.75	
peak electric field	E_{peak}	48	MV/m
emitted energy	$_r$	1	uJ
central frequency	f_c	8.53	THz
relative bandwidth FWHM	$\Delta\omega/\omega$	143%	

8. X-RAY SOURCE: OPTIONAL

There is no X-ray source in the baseline design but a narrowband emitter suitable for X-ray diffraction can be installed upon users' request. Therefore, here we describe the parameters of the X-ray source that can be built in for studying the atomic structures of the samples in question and complementing the results obtained with THz and/or optical probing. We studied several options for the generation of narrowband X-ray radiation with as high brilliance as possible while keeping the size feasible for a small scale facility. Specifically, we looked into the generation of X-rays with channeling and parametric radiation, bremsstrahlung with filtering and Compton backscattering. The characteristics of the later turned out to be superior and are discussed in some details below.

8.1 Energy of scattered photons

The scattering of 1 um laser radiation on an electron bunch with an energy tunable from 10 to 20 MeV results in X-ray photons in the range from 1.8 to 7.5 keV, which is suitable for X-ray diffraction studies, see Fig. A.

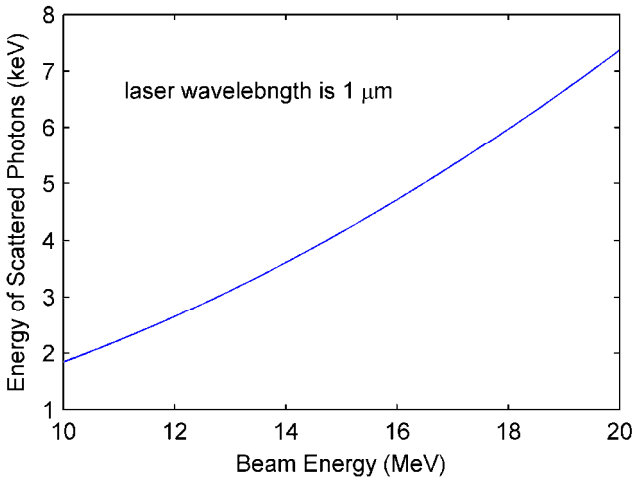

Fig A. The energy of scattered photons vs electron beam energy for a pump laser with a wavelength of 1 um. The beam-laser collision is head-on.

8.2 Number of scattered photons, brilliance

The *total* number of scattered photons and *on-axis* average flux into 0.1% bandwidth is [6,7]

$$N_{ph} = \frac{N_e N_L \sigma_T}{2\pi(\sigma_L^2 + \sigma_e^2)} FF, \qquad = 1.5 \times 10^{-3} f_L N_{ph}.$$

Here, $\sigma_T = (8\pi/3) r_e^2$ is the Thompson scattering cross-section, other symbols are defined in the table below. The term *FF* is a form factor less than unity that depends on rms pulse durations of laser and electron beams, beam spot sizes at the interaction point for the laser and electron beams. It represents the degradation of the interaction efficiency for cases where the pulse durations exceed the interaction diffraction lengths of the laser and electron beams. In what follows *FF* is taken as unity. A large geometric emittance of the electron bunch is the main dominant degradation factor of the spectral brilliance, so the formulas for the average and peak *on-axis* brilliance can be simplified to [6]

$$B_{aver} = \frac{\gamma^2}{4\pi\epsilon_n^2}, \qquad B_{peak} = \frac{\gamma^2}{4\pi\epsilon_n^2} \frac{1}{\tau_b f_L}.$$

Table: Parameters of the Compton backscattering source.

Parameter	Symbol	Value	Units
bunch charge	Q_b	100	pC
number of electrons	N_e	$6.24\ 10^8$	
bunch duration	τ_b	100	fs
e-bunch emittance	ϵ_n	2	mm mrad
rms e-bunch size	σ_e	60	um
geometrical beta-function	β_g	3.5	cm
laser wavelength	λ_L	1	um
rms laser beam size	σ_L	57	um
Rayleigh length	z_R	1	cm
laser pulse energy	$_L$	1	mJ
laser rep. rate	f_L	5	kHz
average power of the laser		6	W
number of scattered photons at all angles/per shot	N_{ph}	$5\ 10^3$	
total number of photons per second		$2.5\ 10^7$	
peak brilliance	B_p	$3.6\ 10^{14}$	ph/s/mm^2/mrad^2/0.1%BW
average brilliance	B_{av}	$3.6\ 10^5$	ph/s/mm^2/mrad^2/0.1%BW

8.3 The laser

For estimates we use the parameters of an off-the-shelf laser called PHAROS [8]. It is quite suitable as a pump for the Compton source. The pulse duration down is to 190 fs, which is a bit too long for pump-probe experiments but good enough for estimates. The dependence of the pulse energy on the repetition rate for this laser is given in Fig. B. The detailed quantitative description can be found in the Table A. It is interesting to note that several laser systems can be combined to deliver up to 60 W of average power.

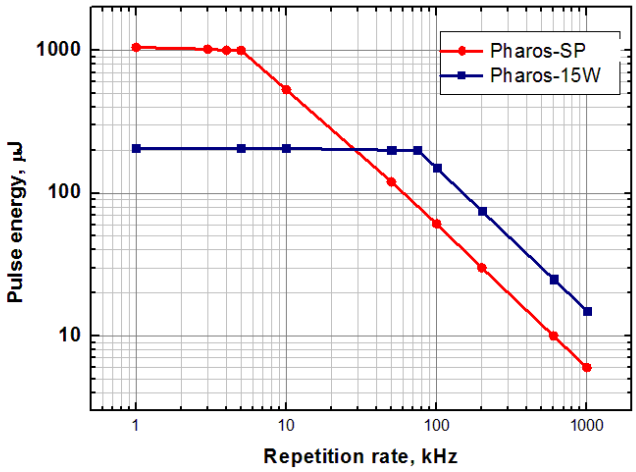

Fig B: Pulse energy vs. repetition rate for the commercial lasers from 'Light Conversion.'

Table A: Parameters of the PHAROS lasers

Model	PHAROS-4W	PHAROS-6W	PHAROS-10W	PHAROS-15W	PHAROS SP	PHAROS SP 1.5	PHAROS 2mJ	PHAROS LP
Max. average power	4 W	6 W	10 W	15 W	6 W		6 W	18 W
Pulse duration (assuming Gaussian pulse shape)	290 fs				190 fs		300 fs	10 ps
Pulse duration range	290 fs – 10 ps				190 fs – 10 ps		300 fs – 10 ps	10 ps
Max. pulse energy	> 0.2 mJ				> 1.0 mJ	> 1.5 mJ	> 2 mJ	> 30 µJ
Beam quality	TEM_{00}; $M^2 < 1.2$			TEM_{00}; $M^2 < 1.3$				TEM_{00}; $M^2 < 1.2$
Repetition rate	Single pulse – 200 kHz (extendable to 1 MHz)							600 kHz
Centre wavelength	1028 nm ± 5 nm							
Output pulse stability	< 0.5 % rms over 24 hours *							
Pre-pulse contrast	< 1 : 1000 **							
Post-pulse contrast	< 1 : 200							
Polarization	Linear, horizontal							
Beam pointing stability	< 20 µrad/°C							
Beam divergence	1.1x diffraction limited (of $M^2 < 1.2$ or $M^2 < 1.3$ beam)							
Burst output	Pulse burst output on trigger signal. Every n^{th} pulse continuous or trigger controlled output (pulse temporal spacing in burst corresponds to amplifier repetition rate)							
Oscillator output	Optional, typical output 0.5–1 W, 76 MHz, < 100 fs							

8.4 Energy spread of scattered photons

The basic sources of energy spread in scattered photons are energy spread in an electron bunch, laser bandwidth and divergence of the laser and electron beams at the collision point. For a head-on collision, the total energy spread reads [9]

$$\left.\frac{\Delta\omega_s}{\omega_s}\right|_{\theta_{x0}=0,\theta=0} \approx \sqrt{\frac{\gamma^4(\Delta\xi_{xe}^2+\Delta\xi_{ye}^2)^2}{4}+4\frac{\Delta\gamma^2}{\gamma^2}+\left(\frac{\Delta\xi_{xL}^2+\Delta\xi_{yL}^2+\Delta\xi_{xe}^2+\Delta\xi_{ye}^2}{8}\right)^2+\frac{\Delta\omega_0^2}{\omega_0^2}}.$$

Here, $\Delta\gamma$ is the bunch energy spread, $\Delta\omega$ is the laser bandwidth, $\Delta\xi$ is the angular divergence of a laser or electron beam. Let us estimate each term one by one. The relative laser bandwidth can be re-written as

$$\frac{\Delta\omega}{\omega}=\frac{\lambda}{\pi l_L},$$

and for the PHAROS laser with a pulse duration of 190 fs and the central wavelength 1 um is just 0.0056. If a 10 um laser is used with the same pulse duration, then this ratio yields 0.056. The long wavelength laser pulses have ten times more photons but the gain in the number of photons is cancelled out by the dramatically increased bandwidth.

The maximum energy spread of the electron is planned to be limited to 1%, so it will give 2% of energy spread of photons. The divergence of a laser beam is

$$\Delta\xi = \frac{\lambda}{\pi w_0},$$

where $w_0 = 2\sigma_L$ is the laser spot size at the waist, and for the parameters above $\Delta\xi = 0.0028$. The divergence of an electron beam is

$$\Delta\xi = 2\frac{\epsilon}{\sigma},$$

where ϵ is the geometric emittance and σ is the beam size at the waist. For a 10 MeV e-bunch, the bunch divergence is 0.0067.

Plugging all the numbers into the formula at the beginning of this paragraph gives the total energy spread of scattered photons of 2.1%. Therefore, the total number of photons scattered per second into 0.1% BW is 1.2 10^6.

8.5 Optical laser for optical pump –THz probe experiments and Compton source

One should keep in mind that there is a need for an optical laser for optical pump –THz probe experiments, and it is advantageous to have an optical parametric amplifier (OPA) so one can cover some frequency range. The tuning range of the possible OPA is shown below, and it uses of the same PHAROS laser mentioned above. Thus, the same laser can be used as a pump for the Compton source and OPA. The whole laser system requires 0.5 m^2 as it is shown in Figs. below.

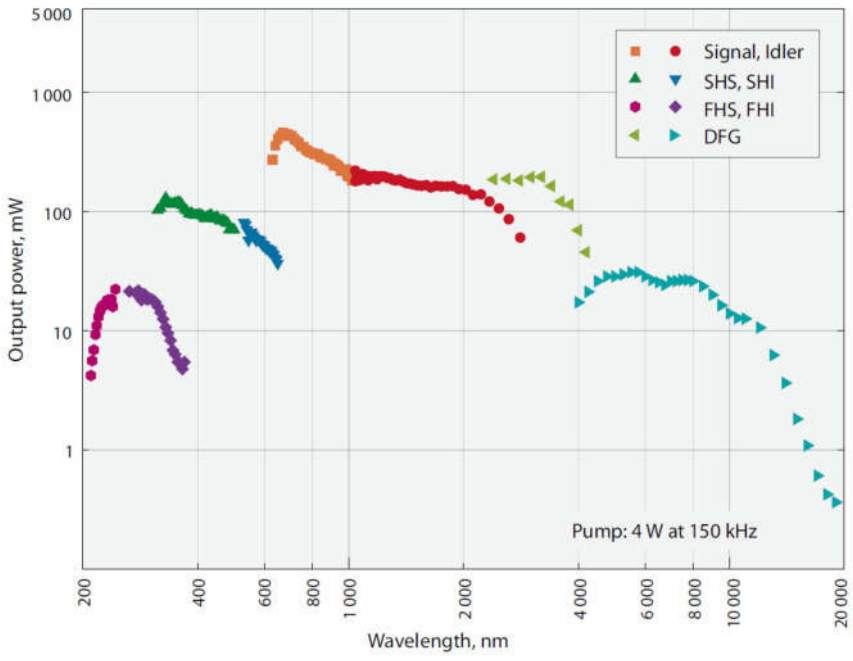

Typical tuning curve of ORPHEUS

Compact layout of PHAROS pump laser in tandem with ORPHEUS
on 0.5 square meter

SUMMARY

The proposed THz Light Source will deliver quasi-half-cycle or multi-cycle THz pulses with a field strength in the V/Å range at a multi-kilohertz repetition rate. The source is flexible and has a number of *unique features*:

- with respect to other THz-FELs, it will be the source machine designed specifically for pump-probe experiments;
- will cover the range from 5 to 15 THz where laser-based THz sources fail to work;
- will generate quasi-half-cycle pulses with the field strength and repetition rate that are far beyond of any existing or planned source.

REREFENCES:

1 Tanaka, Takashi. "Proposal to Generate an Isolated Monocycle X-Ray Pulse by Counteracting the Slippage Effect in Free-Electron Lasers." Physical review letters 114.4 (2015): 044801.
2 Fülöp, J. A. et al., (2012). Generation of sub-mJ terahertz pulses by optical rectification. Optics letters, 37(4), 557-559.
3 Oh, T. I. et al., (2013). Intense terahertz generation in twocolor laser filamentation: energy scaling with terawatt laser systems. New Journal of Physics, 15(7), 075002
4 Wu, Z. *et al.*, (2014, September). THz light source at SLAC FACET user facility. In Infrared, Millimeter, and Terahertz waves (IRMMW-THz), 2014 39th International Conference on (pp. 1-2). IEEE.

5 Vinokurov, N. A., Jeong, Y. U. (2013). Generating High-Power Short Terahertz Electromagnetic Pulses with a Multifoil Radiator. Physical review letters, 110(6), 064805.

6 Krafft, Geoffrey A., and Gerd Priebe. "Compton sources of electromagnetic radiation." *Reviews of Accelerator Science and Technology* 3.01 (2010): 147-163.

7 Graves, W.S. et al. “MIT inverse Compton source concept.” Nuclear Instruments and Methods in Physics Research Section A: Accelerators, Spectrometers, Detectors and Associated Equipment 608.1 (2009): S103-S105.

8 http://www.lightcon.com/products/product.php?ID=28

9 Brown, Winthrop J., and Frederic V. Hartemann. "Three-dimensional time and frequency-domain theory of femtosecond x-ray pulse generation through Thomson scattering." *Physical Review Special Topics-Accelerators and Beams* 7.6 (2004): 060703.